Pressure-induced elastic softening of monocrystalline zirconium tungstate at 300 K

C. Pantea,[1] A. Migliori,[1] P. B. Littlewood,[2,3] Y. Zhao,[1] H. Ledbetter,[1] J. C. Lashley,[1] T. Kimura,[1] J. Van Duijn,[4] and G. R. Kowach[5,*]

[1]*Los Alamos National Laboratory, Los Alamos, New Mexico 87545, USA*
[2]*Cavendish Laboratory, University of Cambridge, Madingley Road, Cambridge CB3 OHE, United Kingdom*
[3]*National High Magnetic Field Laboratory, Tallahassee, Florida 32310, USA*
[4]*Department of Physics and Astronomy, Johns Hopkins University, Baltimore, Maryland 21218, USA*
[5]*Bell Laboratories, Lucent Technologies, Murray Hill, New Jersey 07974, USA*

(Received 29 March 2006; published 29 June 2006)

The elastic tensor of monocrystalline ZrW_2O_8 was determined near 300 K as a function of pressure, using pulse-echo ultrasound in a large-volume moissanite anvil cell. An unusual decrease in bulk modulus with increased pressure was observed. A framework-solid-based nonlinear model with many degrees of freedom predicts the observed behavior. We also observe that ReO_3, a similar framework solid but lacking the necessary degrees of freedom, fails to display softening. Additionally, the pressure-induced phase transition from α-ZrW_2O_8 (cubic) to γ-ZrW_2O_8 (orthorhombic) is found to take place at $\approx$0.5 GPa, a result confirmed by Raman spectroscopy.

DOI: 10.1103/PhysRevB.73.214118 PACS number(s): 62.20.Dc, 62.50.+p, 64.70.−p

The negative-thermal-expansion (NTE) compound ZrW_2O_8 has been well studied because it remains cubic with a nearly constant NTE coefficient throughout its region of existence.[1] Despite the NTE, but like most solids, its elastic moduli soften on warming.[2] This observation goes against conventional thought because as ZrW_2O_8 is warmed, its volume decreases just as if pressure were applied, and most solids *stiffen* when compressed. Using pulse-echo ultrasound in a large-volume moissanite anvil cell,[3] we have determined the complete elastic tensor of monocrystalline ZrW_2O_8 near 300 K as a function of pressure and found that ZrW_2O_8 softens when compressed, then undergoes a phase transition at 0.5 GPa, a much higher pressure than previously reported for powdered or unoriented-fragment material.

The pressure-induced phase transition from α-ZrW_2O_8 (cubic) to γ-ZrW_2O_8 (orthorhombic) was determined previously in powder samples[1,4,5] and a monocrystal in a diamond-anvil cell.[6] For this work, several monocrystals of ZrW_2O_8, made using a nonequilibrium technique[7] were used for the measurements reported here. The crystals were colorless, perfectly transparent, and visually defect-free. Optically flat (100) faces were used to measure C_{11} and C_{44}, and (110) faces for $C'=(C_{11}-C_{12})/2$ and $C_L=(C_{11}+C_{12}+2C_{44})/2$ for a total of four separate measurements, providing some redundancy because cubic materials possess only three independent elastic moduli. Monocrystals of ReO_3 were prepared by vapor transport in a Bridgman furnace. The crystals were dark red and were parallelepiped shaped. Back-reflection Laue diffraction showed sharp spots on the faces of the parallelepiped which were determined to be (100) with a lattice constant of 3.752 Å. Sound speed was determined at multiple pressures using an all-digital ultrasonic pulse-echo-overlap method, described elsewhere.[8] The size of the monocrystals was 1–1.5 mm on one side. Specimen length changes were corrected using the low-pressure elastic moduli. The sample was mounted in the 3 mm hole of an Al gasket, with about 3 mm of space between anvils. Pressure was applied with opposing monocrystal SiC (moissanite) anvils (Fig. 1), in a pressure cell designed by one of us (Y.Z.). The pressure-transmitting medium consisted of a mixture of hexagonal boron nitride[9] and fluorinert.[10] A thin acoustically transparent bond between anvil and sample was achieved with cyanoacrylate adhesive, a low-bulk-modulus material. Pressure was determined using ruby fluorescence.[11] We used

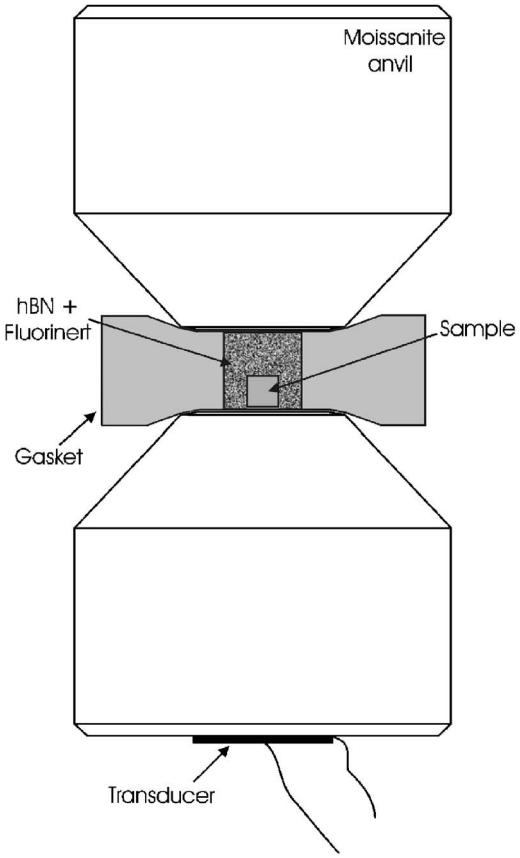

FIG. 1. Schematic of the high-pressure SiC anvil cell used for determination of elastic moduli at high pressure.

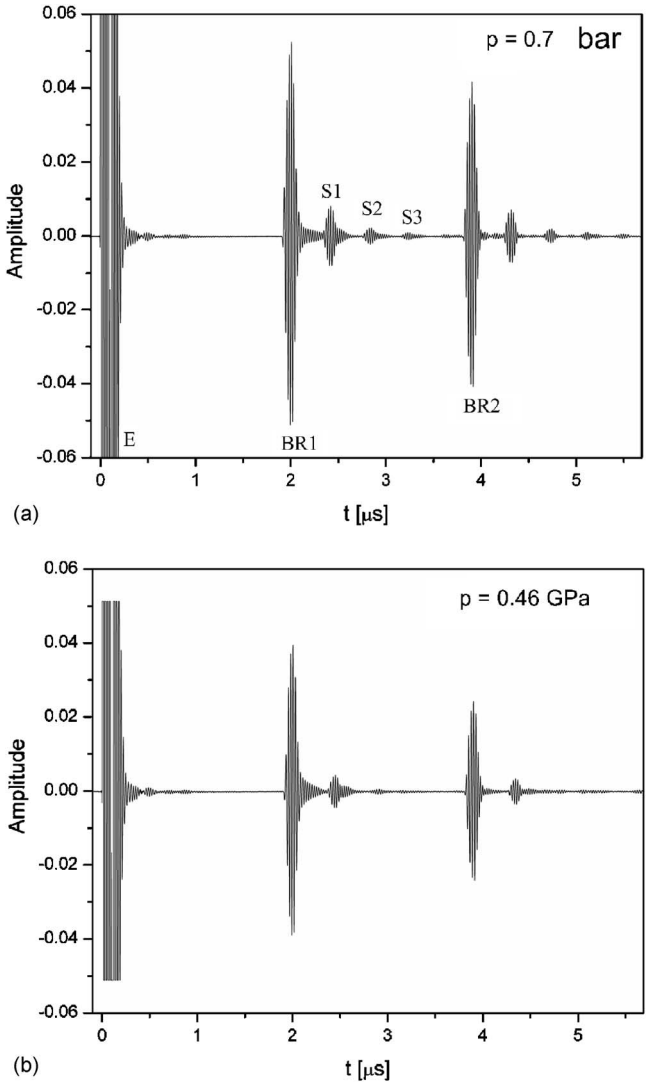

FIG. 2. Acoustic signal at two pressures in the high-pressure system for determination of C'. (a) Atmospheric pressure (0.7 bar); (b) 0.46 GPa. *E* excitation signal; BR1, first buffer-rod (in our case a SiC anvil) reflection; *Si* ($i=1-3$), *i*th reflection from the sample; BR2, second buffer-rod reflection.

a high-resolution Raman setup consisting of an Ar laser (INNOVA 70C), equipped with an Acton Research Corporation SpectraPro 500i spectrometer (0.500 mm imaging triple-grating monochromator/spectrograph), with a grating of 2400 lines/mm. All elastic moduli were measured in the adiabatic limit. X-ray diffraction measurements by others are in the isothermal limit. The difference between the limits depends on the thermal expansion coefficient, sound speed, and specific heat and is expected to be only a few percent.

Measurements were made from ambient to about 0.71 GPa, spanning the cubic-to-orthorhombic phase transition (0.5 GPa). An example of the quality of the acoustic signal in our system in shown in Fig. 2. Elastic moduli obtained in the pressure cell at atmospheric pressure agree well with previous resonant ultrasound[12] results.[2] In the present study we obtained (all units are in GPa) $C_{11}=127.6$ (Ref. 2, 128.4), $C_{44}=26.2$ (Ref. 2, 27.4), $C'=38.6$ (Ref. 2, 40.4), $C_L=114.3$ (Ref. 2, 115.4), and $B=75.5$ (Ref. 2, 74.5). The changes with pressure in elastic moduli $C_{ij}(P)$ are shown in Fig. 3. We determine the critical pressure for the α-γ transition in ZrW_2O_8, to be 0.5 ± 0.05 GPa, not consistent with previous studies.[1,4–6] Depending on details of the measurement, when pressure is applied to powdered or fragmented material as in all previous work, it can sometimes cause stress risers[13] where, say, the sharp edge of one grain touches the face of another. If this occurs, then the local pressure at the contact point is always higher than the applied hydrostatic pressure, making the onset of a pressure-induced phase transition appear lower and the extent broader. From the details of previously published work, we could not determine if this effect was present.

We observe a sharp phase transition consistent with that expected for high-quality monocrystals. The width of the phase transition is estimated to about 0.1 GPa. Nevertheless, to confirm the critical pressure from elastic moduli, we also measured the Raman spectrum of monocrystal ZrW_2O_8 (Fig. 4) as a function of pressure in the same pressure cell used to measure elastic moduli. We observe only α-ZrW_2O_8 from 0 to 0.46 GPa, with no sign of a second phase appearing. At pressures higher than the critical pressure determined from elastic moduli (0.5 GPa), only γ-ZrW_2O_8 appears. This confirmation is important in establishing that the pronounced softening of C_{11} and the behavior of the other elastic moduli is caused by the underlying physics, and not by a phase transition broadened by a nonideal experiment.

The pressure dependence of C_{11} differs substantially from that of C_{44}, and C'. Because the elastic moduli were determined in four separate runs, small errors in pressure determination for each loading of the pressure cell, especially at the phase transition where the elastic moduli change more rapidly, affect the computed bulk modulus B. To obtain a consistent result, C_{12} was calculated from both C' and C_L, and then the fits for each were forced to extrapolate to a single critical pressure. Remarkably, C' (shear propagation along [110], polarization along $[1\bar{1}0]$) and C_{44} (shear propagation along [100], polarization along [010]), vary weakly and continuously below the critical pressure, consistent with a cubic solid that should exhibit only small changes in the shear moduli as it changes volume because bond angles hardly change. In contrast, all the propagation speeds measured in the high-pressure phase (γ-ZrW_2O_8) were lower than in α-ZrW_2O_8, and increase with pressure, in agreement with results by others[5] [note that the γ-ZrW_2O_8 elastic moduli do not exhibit a simple correspondence to those in α-ZrW_2O_8 because the γ (orthorhombic) phase possesses nine independent elastic moduli in a tripled unit cell; however, propagation speeds remain a good measurement].

One feature of our study seems especially noteworthy in terms of crystal chemistry (structure, bonding, properties): C_{11} (longitudinal propagation along [100], polarization along [100]) and the bulk modulus change excessively, nearly abnormally, as volume decreases, either by pressure or by temperature. To understand these effects, we consider the ZrW_2O_8 crystal structure consisting of a three-dimensional network of corner-linked WO_4 tetrahedra and ZrO_6 octahedra, a 44-atom unit cell. A complete framework-solid analy-

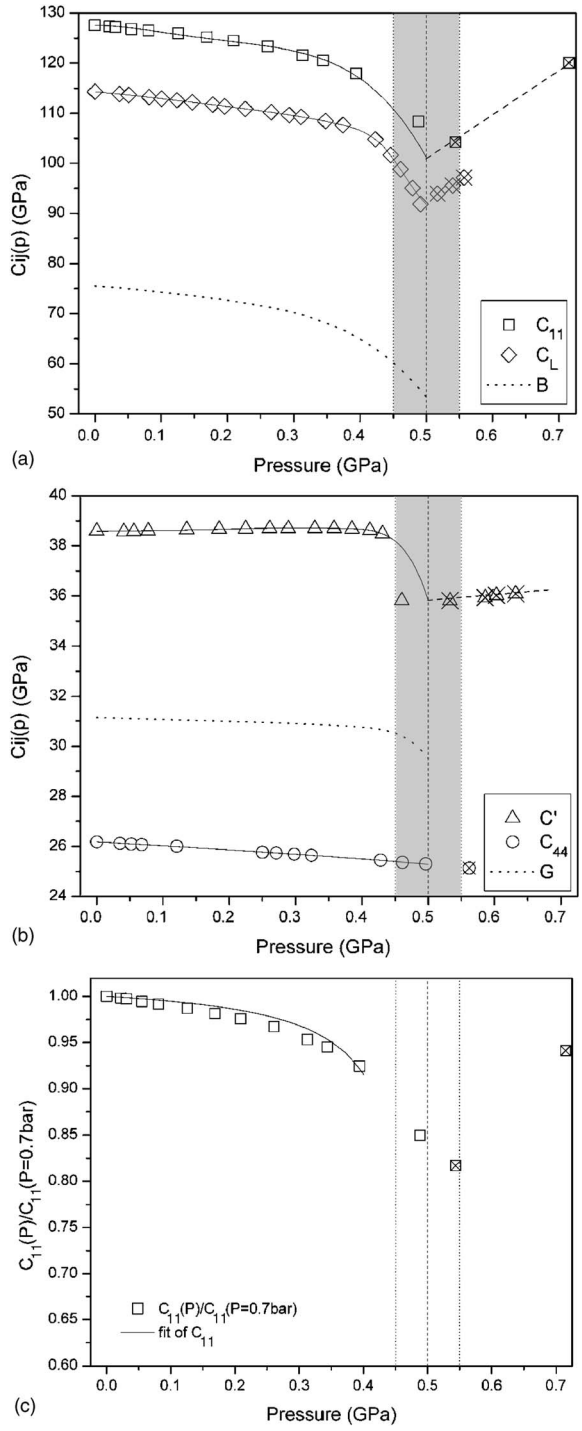

FIG. 3. Elastic moduli of ZrW_2O_8 at 295 K vs pressure. (a) C_{11} and C_L vs pressure. Solid lines, fit of the elastic constants; dotted line, bulk modulus B computed from a smooth fit to the measured elastic moduli (symbols). (b) C' and C_{44} vs pressure. Solid lines, fit of the elastic constants; dotted line, computed shear modulus G. (c) Solid line, fit of C_{11} to Eq. (2). Observations: crosses, measurements in the γ phase of ZrW_2O_8. The acoustic transit times do not correspond to γ-ZrW_2O_8 elastic moduli because the γ (orthorhombic) phase possesses nine independent elastic moduli in a tripled unit cell. However, ρv^2 values for γ-ZrW_2O_8 are shown only to better illustrate the phase transition. The vertical dashed line in (a), (b), and (c) represents the phase-transition pressure.

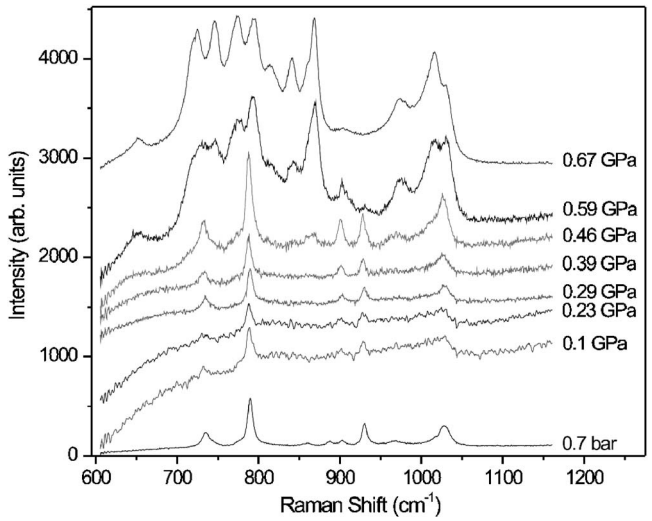

FIG. 4. Raman spectra of ZrW_2O_8 as function of pressure for a 600–1150 cm^{-1} interval.

sis where the tetrahedra and octahedra are considered rigid, and the bond angles perfectly soft, of ZrW_2O_8 by Pryde *et al.*[14] finds that the number of zero-frequency rigid unit modes (RUMs) depends on the 2/3 power of the number of atoms (it is a surface in the first Brillouin zone). Introducing small, linear bond bending stiffness changes the surface to a volume with, therefore, a "thermodynamic" number of quasirigid unit modes (QRUMs), albeit only in the limit of zero amplitude, a problem because NTE requires "large" amplitudes. A similar "constrained lattice" (CL) model with all the essential features (Fig. 5, top right), by Simon and Varma,[15] like the FS analysis of Pryde, is different in an important way from previous work[14] because the "open space" produces many zero-frequency degrees of freedom. Simon and Varma[15] analyze this generalized RUM problem to show that zero-frequency degrees of freedom (RUMs) can exist with large amplitudes of motion, a crucial point for explaining NTE.

Structures with open space, like ZrW_2O_8[5], are intrinsically different from materials like ReO_3,[16] La_2CuO_4[17] or $Lu_5Ir_4Si_{10}$,[18] where effects of the phase transition also extend above and below a critical temperature. Of importance here is that the open lattice structure (lacking in ReO_3, La_2CuO_4, or $Lu_5Ir_4Si_{10}$) combined with an anharmonic bond bending stiffness (lacking in FS and CL models), not the phase transition itself, induces a special pressure signature in ZrW_2O_8. In Fig. 6, we show, as an example, our measurements in the same system described above, of C_{11} for a 0.6-mm-thick monocrystal of ReO_3 as a function of pressure through its phase transition. This framework solid lacks open space and, while it still has a mechanical "buckling transition," fails to display the signature softening of ZrW_2O_8, and has conventional thermal expansion.

To understand the effect of an anharmonic bond bending stiffness, first consider the lattice (Fig. 5, top left) that corresponds to zero tilting, low temperature, high volume, and high bulk modulus B. The right side corresponds to alternately tilted polyhedra, higher temperature, lower volume, and much lower bulk modulus. The key difference between

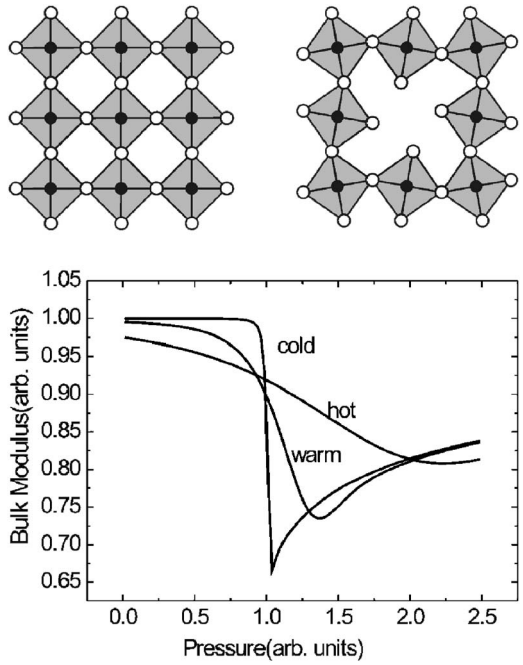

FIG. 5. Top left, a rigid solid like ReO_3, that does not display NTE. Top right, a simple picture of a framework solid showing how approximately rigid structures that twist can reduce volume because the open space is reduced when twisting occurs. The twisting can be either thermal-motion induced or pressure induced. Bottom, variation of bulk modulus with pressure at different temperatures for a nonlinear modified CL model Eq. (2). The three fitting parameters and temperature are arbitrary and chosen to illustrate the characteristic pressure signature that we observe in Fig. 2.

the two is that, as Simon[15] and Pryde[14] show, the missing rigid unit for the lattice on the right makes many thermal distortions possible, while on the left there is only one because once one rigid unit on the left twists, the positions of all the others are determined. Clearly "large" amplitudes and many modes are necessary for NTE. For these pictures, there are two apparent sources of volume-reducing strain. One is

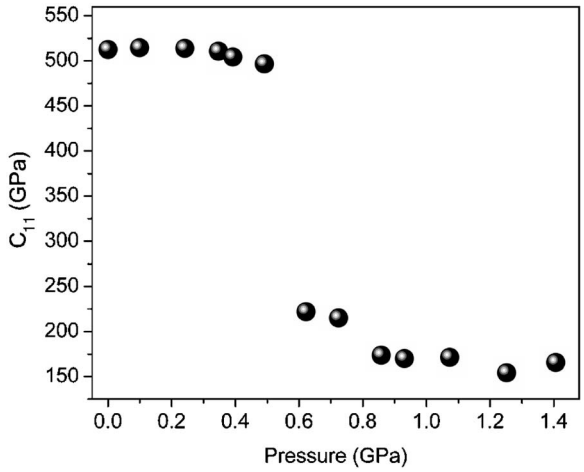

FIG. 6. C_{11} for ReO_3 versus pressure at 295 K. The sample was a monocrystal 0.6 mm thick. Measurements were performed in the same system as for ZrW_2O_8.

the ordinary stiffness of an isolated octahedron (assumed infinite in the CL model); the other arises from tilting and flexing of semirigid structures and near-zero-stiffness linear bonds (QRUMs). However, low-frequency linear modes are not consistent with our observed pressure dependence of the elastic moduli. A purely nonlinear bond bending stiffness, described below, for this second strain mechanism suggests a source for the pressure-induced softening of the bulk modulus B, the monocrystal stiffness C_{11}, and indeed all the dilatation-related elastic moduli while predicting that the magnitude of the thermal expansivity β will increase with pressure, in contrast to the usual decrease that follows from thermodynamics.

It remains to determine the expected pressure dependence of C_{11} based on the modifications to the CL and FS models. We use the framework solid of Fig. 5 (top right) to construct a local energy E that has as the order parameter θ the octahedral tilt angle such that

$$E = \sum_i [p(1 - \cos\theta_i) + K\theta_i^2/2 + \gamma\theta_i^4/4 + \delta\theta_i^6/6 + \cdots]. \tag{1}$$

Here K is the bond-angle stiffness, and p is pressure, and the subscript represents the (extensive) independent degrees of freedom. At zero temperature, the minima for this free energy are zero bond angles below a critical pressure, nonzero above. Using this energy to construct a partition function from which we compute $\langle\theta^2\rangle$, and noting that the framework solid makes $\langle\theta^2\rangle$ proportional to the decrease in volume δV, we may compute the bulk modulus, here adding in parallel a constant term from the bond-length stiffness. A schematic of the results is shown in Fig. 5 (bottom), at three different temperatures, chosen for this model to showcase the qualitative effect of temperature. At $T=0$, the result is just that from a mechanical instability—the Euler strut—where the modulus jumps down at the critical pressure, and recovers slowly (in a way determined by the form of the local potential). This is the result that we expect for any overconstrained model of coupled octahedra. At a nonzero temperature and small pressures, the fluctuations near the instability lead to additional modulus softening at low pressures and a volume decrease near zero pressure of the form

$$\frac{\delta C_{11}}{C_{11}} \approx \frac{C_{11}}{P_c}\frac{\delta V}{V} \approx C_{11}\frac{Ak_BT}{P_c^2} \tag{2}$$

well below the critical pressure P_c, where A is a fitting constant. We also show a fit of Eq. (2) in Fig. 3(c). This model not only predicts strong softening of the elastic moduli, but also predicts NTE of the same order as observed and with linear proportionality to temperature.

The results obtained above cannot be obtained in any limit of the parameters of a harmonic model as a perturbative expansion about them. The constraints lead to a qualitatively new class of properties. These properties are preserved if we generalize the rigid units in Fig. 5 to a polymer, i.e., to chains formed of fixed-length sticks which are deformable in the mutual orientation at the connecting points.

The constrained-lattice model, therefore, explains NTE directly, but also predicts quantitatively why ZrW_2O_8 softens when its volume is decreased via either NTE and warming, or application of pressure, and why ReO_3 (Fig. 5, top left) does not. Essential features of the model include rigid or constrained structures, weak anharmonic bending stiffness between the structures, and open space that permits a "thermodynamic number" of degrees of freedom.

*Present address: Department of Chemistry, The City College of New York, The City University of New York, 138th St. and Covent Ave., New York, NY 10031, USA.

[1] J. S. O. Evans, Z. Hu, J. D. Jorgensen, D. N. Argyriou, S. Short, and A. W. Sleight, Science **275**, 61 (1997).
[2] F. R. Drymiotis, H. Ledbetter, G. B. Betts, T. Kimura, J. C. Lashley, A. Migliori, A. P. Ramirez, G. R. Kowach, and J. van Duijn, Phys. Rev. Lett. **93**, 025502 (2004).
[3] Y. Zhao, LANL Report No. LA-UR-03-3014, 2003 (unpublished).
[4] J. M. Gallardo-Amores, U. Amador, E. Moran, and M. A. Alario-Franco, Int. J. Inorg. Mater. **2**, 123 (2000).
[5] J. D. Jorgensen, H. Zu, S. Teslic, D. N. Argyriou, S. Short, J. S. O. Evans, and A. W. Sleight, Phys. Rev. B **59**, 215 (1999).
[6] T. R. Ravindran, A. K. Arora, and T. A. Mary, Phys. Rev. Lett. **84**, 3879 (2000).
[7] G. R. Kowach, J. Cryst. Growth **212**, 167 (2000).
[8] C. Pantea, J. D. Jorgensen, S. Teslic, S. Short, D. N. Argyriou, J. S. O. Evans, and A. W. Sleight, Rev. Sci. Instrum. **76**, 114902 (2005).
[9] H. T. Hall, *Metallurgy at High Pressures and High Temperatures* (Gordon and Breach, New York, 1964), pp. 144–179.
[10] T. Varga, A. P. Wilkinson, and R. J. Angel, Rev. Sci. Instrum. **74**, 4564 (2003).
[11] H. K. Mao, J. Xu, and P. M. Bell, J. Geophys. Res. **91**, 4673 (1986).
[12] A. Migliori and J. Sarrao, *Resonant Ultrasound Spectroscopy* (Wiley, New York, 1997).
[13] Z. Hu, D. G. Rickel, A. Migliori, R. G. Leisure, J. Zhang, Y. Zhao, S. El-Khatib, and B. Li, Physica B **241-243**, 370 (1998).
[14] A. K. A. Pryde, K. D. Hammonds, M. T. Dove, V. Heine, J. D. Gale, and M. C. Warren, J. Phys.: Condens. Matter **8**, 10973 (1996).
[15] M. E. Simon and C. M. Varma, Phys. Rev. Lett. **86**, 1781 (2001).
[16] J.-E. Jorgensen, J. S. Olsen, and L. Gerward, J. Appl. Crystallogr. **33**, 279 (2000).
[17] A. Migliori *et al.*, Phys. Rev. B **41**, 2098 (1990).
[18] J. B. Betts, A. Migliori, G. S. Boebinger, H. Ledbetter, F. Galli, and J. A. Mydosh, Phys. Rev. B **66**, 060106(R) (2002).